https://doi.org/10.5194/angeo-2021-41
Preprint. Discussion started: 1 September 2021


Annales Geophysicae Discussions
Open Access
EGU

# Estimation of date and magnitude of four major earthquakes using integration of precursors obtained from remote sensing data

Mohammad Mahdi Khoshgoftar[1]* and Mohammad Reza Saradjian[1]

[1] School of Surveying and Geospatial Engineering, College of Engineering, University of Tehran, Tehran, Iran

*Corresponding author: E-mail: mm.khoshgoftaar@ut.ac.ir.

**Abstract:** A single precursor is not usually an accurate, precise and adequate measure to predict earthquake parameters. Therefore, it is more appropriate to exploit parameters extracted from several other single precursors, so that their simultaneous combinations may reduce the uncertainty of the prediction. In this study, remote sensing observations in different modalities acquired from several days before impending earthquakes have been investigated to extract earthquake parameters. They are observations in electron and ion density, electron temperature, Total Electron Content (TEC), Land Surface Temperature (LST), Sea Surface Temperature (SST), Aerosol Optical Depth (AOD), and Surface Latent Heat Flux (SLHF). Regarding the ionospheric precursors, the geomagnetic indices Dst, Kp, Ap and F10.7 were used to detect pre-earthquake disturbances from frequent anomalies associated with geomagnetic activity. In this study, three methods of median, support vector regression (SVR) and random forest (RF) have been used to detect anomalies. When anomalies associated with impending earthquakes are detected, the number of prior days associated with the earthquake is estimated based on the type of precursor. Then, by estimation of the amount of anomaly deviation from the normal state, the magnitude of the impending earthquake is estimated. The final earthquake parameters (such as date and magnitude) can be obtained by integrating the earthquake parameters extracted from different earthquake precursors using mean square error (MSE) method.

**Keywords**: Earthquake, anomaly detection, remote sensing

## 1 Introduction

When an earthquake is happening, energy transmission is generated due the destructive effects of the earthquakes to the environment. The occurrence of these changes before and/or after the earthquake may have various physical and chemical effects on lithosphere, atmosphere and ionosphere making the earthquake more accurately predictable. The abnormal variations in lithospheric, atmospheric and ionospheric parameters are taken as "earthquake precursors". They serve as alarms for impending earthquakes. Many studies have been carried out on earthquake predictions using precursors in lithosphere, atmosphere and ionosphere. The problem arise when some of these major abnormalities may not appear on occasion an earthquake. There are several studies based on the observation of the seismic Lithosphere Atmosphere Ionosphere Coupling (LAIC) anomalies which confirm that the anomalies begin several days before the earthquake and remain a few days after. None of the earthquake precursors can be used alone as an accurate and independent parameter for estimating earthquake parameters without generating some level of uncertainty. Hence, it is necessary to integrate different types of earthquake predictors or earthquake precursors. By integrating a variety of earthquake parameters extracted from different precursors, a more accurate and suitable estimation of final earthquake parameters may be obtained.

Recent advances in the remote sensing and Earth observation technology have facilitate monitoring the ionosphere, the atmosphere and the Earth's surface using various sensors. Nowadays, researchers investigate the factors and indications of earthquakes in more practical and efficient ways. The most important earthquake precursors relevant to ionospheric anomalies recently studied are changes in ion density, ion temperature, electron density and electron temperature provided by DEMETER satellite data (Berthelier et al. 2006; Lebreton et al. 2006; Parrot et al. 2006; Li and Parrot 2012; Li and Parrot

https://doi.org/10.5194/angeo-2021-41
Preprint. Discussion started: 1 September 2021


Annales Geophysicae Discussions

2013; Tao et al. 2017; Ibanga et al. 2018; Li and Parrot 2018). Ionospheric anomaly studies also include changes in total electron content (TEC) obtained from global positioning receivers (GPS) (Liu et al. 2004; Akhoondzadeh 2013; Parrot et al. 2016; Tao et al. 2017). Regarding the Earth's surface, another useful precursor is thermal anomaly obtainable from land surface temperature (LST) (Ouzounov and Freund 2004; Ouzounov et al. 2006; Tronin 2006; Panda et al. 2007; Saraf et al. 2008; Blackett et.al. 2011; Zoran 2012; Akhoondzadeh 2013; Bhardwaj et al. 2017a; Bhardwaj et al.2017b), and from sea surface temperature (SST) (Dziak et al. 2003; Ouzounov et al.2006; Freund et al. 2009). Other useful precursors are outgoing longwave radiation (OLR) (Ouzounov et al. 2007; Rawatet al. 2011; Eleftheriou et al.2016), surface latent heat flux (SLHF) (Dey and Singh 2003; Cervone et al. 2004; Cervone et al.2006; Pulinets et al. 2006; Pulinets and Ouzounov 2011; Zhang et al. 2013; MansouriDaneshvar et al. 2014; Qin et al.2014), and atmospheric anomaly in the form of aerosol optical depth (AOD) (Freund et al. 2009; Akhoondzadeh, 2015; Ganguly 2016; Akhoondzadeh, 2018).

## 2 Data

According to the objective of this study, the data used have been chosen from multiple sources which are as follows:

### 2.1 DEMETER Data

The French micro-satellite DEMETER was launched in June 2004and its scientific mission stopped on 9th of December 2010. The data provided by DEMETER is used to investigate the ionospheric disturbances due to seismic activity, (Parrot et al. 2006). The DEMETER satellite collected its ionospheric parameters related to seismic activities using five sensors. The sensors are Instrument Champ Eletrique (ICE), Instrument Magnetic Search Coil (IMSC), Instrument Detecteur de Partcules (IDP), Instrument Analyseur Plasma (IAP), and Instrument Sonde de Longmuir (ISL). In this study, the ion density ($cm^{-3}$) and temperature (K), and also electron density($cm^{-3}$) and temperature(K) data were collected from ISL and IAP sensors. DEMETER satellite data is available via: http://demeter.cnrs-orleans.fr/.

### 2.2 TEC Data

The most popular product to analyse the ionosphere state is the global ionosphere maps (GIM) of the Total Electron Content (TEC) provided by NASA (National Aeronautics and Space Administration) in the IONEX format (Schaer et al. 1998). The GIM-TEC covers ± 87.5 of latitude and ± 180 of longitude with the spatial resolution of 2.5and 5.0, respectively, and with cadence of 2h. In this study, the 60-day TEC data according to any given geographic location of the earthquakes have been analysed. The GIM-TEC map is obtained from the website https://cddis.nasa.gov/archive/gnss/products/ionex/.

### 2.3 MODIS Data

Two products of Moderate Resolution Imaging Spectroradiometer (MODIS) satellite, i.e., Land Surface Temperature (LST) and Aerosol Optical Depth (AOD) data were used in this study. Both the day/night-time LST images provided by NASA(http://modis.gsfc.nasa.gov/data) were processed. The MODIS Terra and Aqua daily level-3 aerosol product, which is produced by the Dark Target and Deep Blue algorithms and is called ‘‘Aerosol Optical Depth at 550 nm”, is available via: https://giovanni.gsfc.nasa.gov/giovanni/.

### 2.4 OMI Data

In this study, a product of Ozone Monitoring Instrument (OMI), namely Aerosol Optical Depth 483.5 nm has been used. OMI onboard the EOS Aura platform is the continuation of TOMS (Total Ozone Mapping) for total ozone parameter. The OMI instrument employs hyperspectral imaging in push-broom mode to observe solar backscatter radiation in visible and

https://doi.org/10.5194/angeo-2021-41
Preprint. Discussion started: 1 September 2021


Annales Geophysicae Discussions

ultraviolet. Its spatial resolution is 0.25° Lat×0.25° Lon. The OMI products are available via: https://giovanni.gsfc.nasa.gov/giovanni/.

### 2.5 AVHRR Data

Two products of AVHRR (Advanced Very High Resolution Radiometer)including Sea Surface Temperature (SST) and Surface Latent Heat Flux (SLHF) data have been used in this study. Sea surface temperature (SST) anomaly can be related to near coastal seismic activity (Ouzounov and Freund, 2004), but conditions and currents can strongly affect SST. Due to a large thermal inertia of the seawater, its temperature changes more slowly; therefore, in the case of the SST anomalies, some mechanisms of LST anomalies are not applicable (Jiao et al. 2018). The NOAA 0.25° daily Optimum Interpolation Sea Surface Temperature (OISST) is an analysis constructed by combining observations from different platforms (satellites, ships, buoys) on a regular global grid. A spatially complete SST map is produced by interpolating to fill in gaps. The SLHF products are available via:https://psl.noaa.gov/data/gridded/data.noaa.oisst.v2.highres.html.

SLHF is ($Wm^{-2}$) the heat flux absorbed or released by the phase transition (i.e., condensation, evaporation, and melting) of water from the Earth's surface to the atmosphere (Jiao et al. 2018). SLHF is one of the important components of Earth's surface energy budget, which is mainly affected by the atmospheric relative humidity, wind speed, surface temperature, and season (Jiao et al. 2018). Due to the underground fluid movement and the interaction among the underground, surface, and atmosphere, the SLHF anomaly that occurs prior to earthquakes is considered (Alvan et al. 2013). The SLHF products are available via:https://psl.noaa.gov/data/gridded/data.ncep.reanalysis.html.

### 2.6 Geomagnetic Indices

The ionospheric parameters measured by satellite are mainly influenced by the geomagnetic storms and geomagnetic field disturbances, particularly in the equatorial and polar regions. However, in the case of an impending Earthquake, it may be affected further more in the form of anomaly. Such anomalies should also be removed. In order to distinguish anomalies caused by seismic activity from anomalies created by geomagnetic and solar activities, the geomagnetic and solar indices i.e. Dst, Kp, Ap, and F10.7acquired from Space Physics Data Facility (SPDF)have been utilized in this study. In conditions where the quiet solar geomagnetic is established (i.e. Kp< 2.5, -20 nT<Dst< 20 nT and F10.7 < 120 SFU) the situation will be regarded as normal. However, if unusual changes are seen in the ionospheric data, it can be considered due to seismic activity.The geomagnetic and solar indices are available through NOAA (https://www.ngdc.noaa.gov/stp/stp.html).

## 3 Method

### 3.1 Anomaly detection method

Anomaly detection is the process of identifying unexpected items or events in data sets, which differ from the norm. Anomaly detection has two basic assumptions: 1) anomalies only occur very rarely in the data, and 2) their features differ from the normal instances significantly. In order to detect anomalies in each set of time series data from remotely sensed precursors, identification of the normal behaviour of the phenomenon is necessary.

#### 3.1.1 Normal behaviour modelling

In order to model time series behaviour, two common machine learning methods namely the Support Vector Regression (SVR) and Random Forest (RF) have been used in this study.

In SVR-based regression solutions, the input vectors are mapped into a higher-dimensional feature space, then by employing a linear regression in the feature space, the input vectors are separated as far apart as possible. In this study, which is operating in a large space, a kernel function is used (Khosravi, Jouybari-Moghaddam, and Sarajian, 2017).

https://doi.org/10.5194/angeo-2021-41
Preprint. Discussion started: 1 September 2021


Annales Geophysicae Discussions Open Access EGU

Random forest algorithm which is a non-parametric machine learning ensemble method, is an extended version of CART (Classification and Regression Trees) model proposed by Breiman (2001). It is based on the information combination method in which a large number of decision trees are generated and then the results of all the trees are combined for prediction (Cutler et al. 2007). The RF is the multitude of regression trees which performs based on the variance of the data (Liaw and Wiener, 2002).

#### 3.1.2 Anomaly detection

In order to detect anomalies, a reasonable range for regular variations in the time series data should be specified. Signals with normal behaviour fluctuate inside both the upper and lower bounds. Signals outside the boundaries will be detected as anomalies. In this study, the median and inter-quartile method is used to determine the upper and lower bounds (Liu et al. 2004).

The upper and lower bounds are determined using the following Eq. (1):

$$\begin{cases} x_{\text{low}} = m - k \times iqr \\ x_{high} = m + k \times iqr \end{cases} \quad (1)$$

where $x_{low}$, $x_{high}$, $m$ and $iqr$ are respectively the lower bound, upper bound, median value and inter-quartile range of $x$. If the signal lies within the range of the upper and lower bounds, the behaviour of the signal is considered as normal. To determine the intense of abnormal behaviour of the signal, the parameter $D_x$ as deviation of $x$ is calculated by Eq. (2):

$$x_{\text{low}} < x < x_{\text{high}} \Rightarrow -k < D_{\text{x}} = \frac{x - M}{IQR} < k \quad (2)$$

If the absolute value of the parameter $D_x$ is greater than $k$ (i.e. $|D_x|>k$), the behaviour of the parameter is regarded as anomalous. Also, the percentage of parameter deviation from the natural state can be calculated using the Eq. (3) (Saradjian and Akhoondzadeh 2011):

$$P = \pm 100 \times ((|D_{\text{x}}| - k)/k) \quad (3)$$

#### 3.1.3 Preliminary parameters estimation

The Earthquake parameters are preliminarily estimated for each of individual precursors. The $D_x$ value obtained from the previous step is relatively suitable parameter for calculating Earthquake magnitude. Saradjian and Akhoondzadeh (2011) showed the relationship between this parameter and the Earthquake magnitude that can be extracted from Table (1).

**[Table (1) near here]**

Also, according to the day when the anomaly is observed, an impending Earthquake's approximate date can be estimated. Based on observations so far, as an average, a 15-day interval in ionospheric and atmospheric precursors, and as an average, a 16-day interval in thermal precursors from the anomaly observation till earthquake day is considered (Saradjian and Akhoondzadeh 2011).

#### 3.1.4 Finalizing parameters estimation method

After the earthquake parameters (i.e. date and magnitude) are estimated through various precursors using the preliminarily Earthquake parameters estimation, the final value of parameters of the earthquake can be estimated by combining their

https://doi.org/10.5194/angeo-2021-41
Preprint. Discussion started: 1 September 2021


Annales Geophysicae Discussions

results using MSE method. In MSE method, the date and magnitude of an earthquake is calculated by Eq. (4) (Wackerly et. al., 2008):

$$MSE = V + (x - M)^2 \quad (4)$$

where $V$ and $M$ are variance and median of the predicted values of the earthquake parameters for all precursors, respectively; and $x$ is earthquake parameter value for any precursor. Any parameter that has a minimum MSE value is considered as the final parameter of the earthquake.

## 4 Case Studies and results

Four major earthquakes with Magnitude Mw>6have been investigated in this study. These earthquakes occurred in Samoa Islands, Sichuan (China), Kermanshah and Bam (Iran). The characteristics of these earthquakes have been presented in Table 2.The ionospheric parameters obtained from the DEMETER and GPS satellites have been studied and analyzed over the relevant periods of time for each earthquake for areas selected according to Dobrovolsky Formula $R = 10^{0.43M}$which relates the size of affected area to the magnitude of the earthquake (Dobrovolsky et al. 1979).The rest of the time series data for other precursors have been acquired for the relevant periods of time for areas of about 2.5×2.5 degrees in size around each epicentre.

**[Table (2) near here]**

### 4.1 Kermanshah Earthquake

In the case study of Kermanshah Earthquake**,** all time series data were provided for the period of 21 September to 21 November 2017.The TEC anomalies associated with Kermanshah earthquake were observed on November 3 and 4 (Table 3). By observing these anomalies, it can be concluded that an earthquake with magnitude ranging from 7 to 8Mw between November 4 and 19, 2017 would have happened (Fig. 1(d)).

**[Table (3) near here]**

By investigating the Terra day-time LST (°C) anomalies, the minimum value of -3.2°C on October19indicates an earthquake between December 20 and November 4 with Mw>8 would have happened (Fig. 2(a)).

**[Figure 1. Results of TEC Analysis using median for Kermanshah earthquake. The earthquake time is indicated by an asterisk. (a) TEC variations, (b) DTEC, (c) Detected anomalies without considering the solar-magnetic indices, (d) Detected anomalies with considering the solar-magnetic indices.]**

The anomaly observed in the AOD data obtained from the OMI sensor, with a maximum of 370.96% on October 26, 2017, indicates an impending earthquake with *Mw*>8 between October 27 and November 10 (Fig. 2(b)). Also, the estimated earthquake magnitude for the observed anomaly on October 31, 2017 related to the AOD precursor obtained from the Terra and Aqua sensors would be greater than 8*Mw* (Fig. 2(c) & (d)).

**[Table (4) near here]**

By investigating the changes in SLHF, a sharp increase of 346.46%, 117.38% and 288.4% have been observed on 3, 5 and 6 November, respectively (Fig. 2(e)). Due to these anomalies, it can be predicted that an earthquake with magnitude more than 8 Mw will occur in the region.

The results obtained by SVR and Random Forest methods can be found in tables 4 and 5, respectively.

**[Table (5) near here]**

In the case study of Kermanshah, the earthquake parameters deduced based on median from the different precursors using the MSE method indicate that an earthquake would occur between November 4 and 19 with a magnitude more than 8 Mw

https://doi.org/10.5194/angeo-2021-41
Preprint. Discussion started: 1 September 2021


Annales Geophysicae Discussions

(Table 15). Also by using MSE method for the obtained results from both SVR and RF methods, the predicted magnitude of earthquake will be from 7 to 8 Mw between November 4 and 18, 2017 (Table 15).

**[Figure 2. Results of (a) Daytime LST data (Terra, MODIS), (b) AOD data (OMI), (c) AOD (Aqua, MODIS), (d) AOD (Terra, MODIS), (e) SLHF (NOAA), analysis using median method for Kermanshah earthquake. The earthquake day is displayed as a vertical dotted line. The green horizontal lines indicate the higher and lower bounds. The blue line indicates the median value.]**

### 4.2 Samoa Earthquake

For the Samoa earthquake, the time series data of precursors were provided for the period of 21 August to 21 October 2009.TEC anomaly fluctuations began on September 18. The estimated magnitude of the Earthquake for this anomaly would have been between 7 and 8Mwhappening between September 19 and October 3. Anomalies have also been observed on September 25 and 28, 2009 implying that an Earthquake with magnitude $7<Mw<8$ would be expected to happen (Fig. 3(d)).

**[Table (6) near here]**

The data on the changes in total ion density, electron and ion density and electron temperature recorded by DEMETER IAP and ISL sensors for Samoa Earthquake are given in Table 6. The data were recorded when the satellite's orbits were near the epicentre of the Earthquake (i.e. less than 1500 km). With an increase in total ion density observed around 10:30 local time on 25 September, 2009, it was expected that an Earthquake with magnitude between 7 and 8*Mw* would occur between 26 December and 10 October, 2009 (Fig. 4(a)). Also, the changes in electron density showed unusual behaviour. These changes peaked around 10:30 am local time and exceeded 39.37% upper bound on September 25, 2009 (Fig. 4(b)). The ion density anomaly was observed around 10:30 local time on September 25, 2009. For $D_x$ = 2.66, the magnitude of the impending Earthquake is estimated to be between 7 and 8*Mw*thatwould have happened between September 26 and December 10, 2009(Fig. 4(c)). An unusual increase in electron density was observed around 22:30 local time on September 24, 2009(Fig. 4(d)). For this anomaly, an Earthquake with magnitude ranging from7 to 8*Mw* would be expected to happen between September 25 and October 9.

**[Table (7) near here]**

By investigating changes in SST, there were sharp increases of 135.84% and 65.32% on September 6 and 7, 2009, respectively (Fig. 4(g)). The irregularity seen on September 6 indicates that an Earthquake with magnitude greater than *Mw* = 8.0 would have occurred between September 7 and 27.

**[Figure 3. Results of TEC Analysis using median for Samoa earthquake. The earthquake time is indicated by an asterisk. (a) TEC variations, (b) DTEC, (c) Detected anomalies without considering the solar-magnetic indices, (d) Detected anomalies with considering the solar-magnetic indices.]**

The AOD obtained from the OMI sensor shows a maximum anomaly ($D_x$ = 2.56) on September 19, 2009 indicating that an Earthquake with magnitude ranging from 7 to 8 Mw would have happened between September20 and October 4, 2009(Fig. 4(h)).

Unusual AOD changes from the Terra sensor, with a maximum anomaly of 2.07 and 2.08 on August30 and September 21, 2009, respectively indicates that an Earthquake with magnitude ranging from 7 to 8 Mw would have happened (Fig. 4(i)).

The characteristics of detected anomalies using SVR and Random Forest methods are shown in Tables 7 and 8, respectively.

**[Table (8) near here]**

In order to finalize each Earthquake's date and magnitude parameters using the parameters obtained from different precursors, the MSE fusion method has been applied. In the case study of Samoa, according to the MSE method, it was predicted that an Earthquake with magnitude between 7 and 8 Mw would occur between September 25 and October 9, 2009 indicated by both Median and SVR results (Table 15). Based on Random Forest method, the parameters would be the same except for one day earlier starting date (i.e. September 24).

**[Figure 4. Results of (a) Daytime total ion density data (IAP, DEMETER), (b) Daytime electron density data (ISL, DEMETER), (c) Daytime ion density data (ISL, DEMETER), (d) Nighttime electron density data (ISL, DEMETER), (e) Nighttime ion density data (ISL, DEMETER), (f) Nighttime total ion density data (IAP, DEMETER), (g) SST (NOAA), (h) AOD data (OMI), (i) AOD (Terra, MODIS), analysis using median method for Samoa earthquake.]**

https://doi.org/10.5194/angeo-2021-41
Preprint. Discussion started: 1 September 2021


Annales Geophysicae Discussions

### 4.3 Sichuan Earthquake

In the case study of Sichuan Earthquake, all time series data were provided for the period of 21 March to 21 May 2008.Some intense anomalies related to TEC data have been observed on April 21 (6 UTC), May 3 (6 and 18 UTC), and May 9 (10 and 14 UTC) (Fig. 5(d)). These strong anomalies indicate an impending Earthquake with magnitude between 7 and 8Mw. The characteristics of other detected anomalies are seen in Table 9.

**[Table (9) near here]**

The variations of the various parameters extracted from the DEMETER experimental data over the Sichuan region have been presented in Table 9. A sudden and unusual change in ion temperature has been observed three days prior to the Earthquake around 22:30 local time (Fig. 6(a)). This means that an Earthquake with magnitude ranging from 7 to 8 Mw would have occurred between May 10 and 24, 2008. An anomaly has also been observed on May 21, 2008 in electron density around 10:30 local time which implies an impending earthquake as strong as 7 to 8Mw between 22 April and 6 May (Fig. 6(b)). An unusual increase have been observed in ion density (34.17%) around 10:30 local time on April 21, 2008 (Fig. 6(c)) and also, in total ion density of the order of 48.43% at 10:30 local time on May 21, 2008(Fig. 6(d)).

**[Figure 5. Results of TEC Analysis using median for Sichuan earthquake. The earthquake time is indicated by an asterisk. (a) TEC variations, (b) DTEC, (c) Detected anomalies without considering the solar-magnetic indices, (d) Detected anomalies with considering the solar-magnetic indices.]**

The Tables 10 and 11 show the result of anomaly detection by SVR and Random Forest methods, respectively.

**[Table (10) near here]**

By using the MSE method and the combination of the earthquake parameters obtained from different precursors, it was predicted that an earthquake $7<Mw<8$ would have happened between 4 and 18 May 2008 (Table 15). Also, the MSE method for Random Forest method indicates that an Earthquake with the magnitude between 7 to 8 Mw would have been occurred between 4 and 18 May, 2008 and for SVR method with the magnitude ranging from 7 to 8Mw between April 22 and 18, 2008 (Table 15).

**[Table (11) near here]**

**[Figure 6. Results of (a) Nighttime ion temperature data (IAP, DEMETER), (b) Daytime electron density data (ISL, DEMETER), (c) Daytime ion density data (ISL, DEMETER), (d) Daytime total ion density data (IAP, DEMETER), (e) Daytime LST data (Aqua, MODIS), (f) Nighttime LST data (Aqua, MODIS), (g) AOD data (OMI), (h) AOD (Aqua, MODIS), (i) SLHF (NOAA), analysis using median method for Sichuan earthquake.]**

### 4.4 Bam Earthquake

For Bam earthquake, the time series data of precursors derived during the period of 4 November 2003 to 4January 2004.The TEC signal fluctuations exceeded the defined bounds on December 16, 18 and 19, 2003. These anomalies indicate that an Earthquake with the magnitude between 6 and 7Mw would have happened (Fig. 7(d)).

**[Table (12) near here]**

Also, a sudden decrease in temperature was observed in the day-time LST data on December 12 and 13, which indicates that an Earthquake with magnitude ranging from 7 to 8 Mw would have been occurred. By investigating the night-time LST fluctuations, extreme increases in temperature on December 6 and 7, 2003 indicate an Earthquake with magnitude ranging from 6 to 7Mw would have been happened. Moreover, by observing the maximum value of 2.14 on December 6, it can be concluded that an Earthquake with magnitude between 7 and 8 Mw would have happened between December 7 and 22. Unusual change in day time LST data (Terra-MODIS sensor) with the minimum value ($D_x$ = -3.32) occurred on November 30. Due to this anomaly, an Earthquake with $Mw>8$ would have been occurred (Fig. 8(a) to (d)).

**[Table (13) near here]**

https://doi.org/10.5194/angeo-2021-41
Preprint. Discussion started: 1 September 2021


Annales Geophysicae Discussions

Unusual AOD changes on December 12, 2003, with values of 4.51 and 3.42 respectively for the Aqua and Terra sensors indicate an Earthquake with a magnitude greater than 8 *Mw* would have been occurred between December 13 and 27(Fig. 8(e)& (f)).

**[Figure 7. Results of TEC Analysis using median for Bam earthquake. The earthquake time is indicated by an asterisk. (a) TEC variations, (b) DTEC, (c) Detected anomalies without considering the solar-magnetic indices, (d) Detected anomalies with considering the solar-magnetic indices.]**

The anomalies obtained by SVR and Random Forest methods, respectively, are shown in tables 13 and 14.

**[Table (14) near here]**

By combining the predicted parameters obtained from different predictors using the MSE method, it is predicted that an Earthquake would occur between December 13 and 28, 2003, for median anomaly detection method. The combination of anomalies obtained from the SVR and Random Forest by using MSE method predicts an Earthquake between December 16 and 31, 2003 and between December 16 and 30, 2003, respectively. The magnitude of this Earthquake is estimated to be 7<Mw<8 for both median and random forest methods and to be 6<*Mw*<7 for the SVR method (Table 15).

**[Figure 8. Results of (a) Daytime LST data (Aqua, MODIS), (b) Daytime LST data (Terra, MODIS), (c) Nighttime LST data (Aqua, MODIS), (d) Nighttime LST data (Terra, MODIS), (e) AOD data (Aqua, MODIS), (f) AOD (Terra, MODIS), (g) SLHF (NOAA), analysis using median method for Bam earthquake.]**

**[Table (15) near here]**

## 5 Conclusions

Assuming that estimation of Earthquake parameters using each predictor individually is accompanied by some uncertainties, this study considered integrating the capabilities of different earthquake parameters extracted from some of the same earthquake predictors to better estimate earthquake parameters. To identify the anomalous states that may be associated with impending earthquakes, variations of different earthquake precursors have been analysed for four earthquakes by using Median, SVR and Random Forest methods. For each precursors, the date and magnitude were estimated according to the earthquake signals. By integrating the earthquake parameters obtained from all precursors, the final earthquake parameters were estimated more accurately.

Since different precursors have been used to analyse the final earthquake parameters, therefore, for all earthquakes, the estimated earthquake parameters for each earthquake are close to the actually recorded parameters. This can lead to accurate estimation of earthquake parameters with respect to the number and variety of earthquake precursors. Based on the results, it seems that methods such as SVR and Random Forest dealing with nonlinear and complex behaviours of time series are more sensitive than the Median method. Therefore, it can be accounted that these methods are suitable tools for detecting anomalies in nonlinear time series related to changes in seismic precursors.

Since various factors can cause unusual behaviour in different ionospheric, atmospheric or lithospheric parameters, more careful studies should be conducted to distinguish the anomalies caused by the daily changes from anomalies due to seismic activities.

## Acknowledgements

The authors would like to acknowledge LPC2E for the DEMETER data, NASA Jet Propulsion Laboratory for the TEC data and NOAA for the geomagnetic indices, SST and SLHF data. Also analyses and visualizations used in this study were produced with the Giovanni online data system, developed and maintained by the NASA GES DISC.

https://doi.org/10.5194/angeo-2021-41
Preprint. Discussion started: 1 September 2021


Annales Geophysicae Discussions

**Disclosure statement**

There is no conflict of interest between authors.

**References**

Akhoondzadeh, M. (2013). An Adaptive Network-based Fuzzy Inference System for the detection of thermal and TEC anomalies around the time of the Varzeghan, Iran, (Mw D 6.4) earthquake of 11 August 2012. Advances in Space Research 52(5): 837–852. doi:10.1016/j.asr.2013.05.024.

Akhoondzadeh, M.: Ant Colony Optimization detects anomalous aerosol variations associated with the Chile earthquake of 27 February 2010. Advances in Space Research 55(7): 1754–1763. doi:10.1016/j.asr.2015.01.016, 2015.

Akhoondzadeh, M., De Santis, A., Marchetti, D., Piscini, A., &Cianchini, G.: Multi precursors analysis associated with the powerful Ecuador (MW = 7.8) earthquake of 16 April 2016 using Swarm satellites data in conjunction with other multi-platform satellite and ground data. Advances in Space Research 61(1): 248–263. doi:10.1016/j.asr.2017.07.014, 2018.

Alvan, H. V., Azad, F.H.,&Mansor, S.: Latent heat flux and air temperature anomalies along an active fault zone associated with recent Iran earthquakes. Advances in Space Research 52(9): 1678–1687. doi:10.1016/j.asr.2013.08.002, 2013.

Berthelier, J. J., Godefroy, M., Leblanc, F., Seran, E., Peschard, D., Gilbert, P., &Artru, J.: IAP, the thermal plasma analyzer on DEMETER. Planetary and Space Science 54(5): 487–501. doi:10.1016/j.pss.2005.10.018, 2006.

Bhardwaj, A., Singh, S., Sam, L., Bhardwaj, A., Martín-Torres, F.J., Singh, A., & Kumar, R.: MODIS-based estimates of strong snow surface temperature anomaly related to high altitude earthquakes of 2015. Remote Sensing of Environment 188: 1–8. doi:10.1016/j.rse.2016.11.005, 2017a.

Bhardwaj, A., Singh, S., Sam, L., Joshi, P.K., Bhardwaj, A., Martín-Torres, F.J., & Kumar, R.: A review on remotely sensed land surface temperature anomaly as an earthquake precursor. International Journal of Applied Earth Observation and Geoinformation 63: 158–166. doi:10.1016/j.jag.2017.08.002, 2017b.

Blackett, M., Wooster, M.J., &Malamud, B.D.: Exploring land surface temperature earthquake precursors: A focus on the Gujarat (India) earthquake of 2001. Geophysical Research Letters 38 (15). doi:10.1029/2011GL048282.

Breiman, L. (2001). Random forests. Machine Learning, 45(1): 5-32, 2011.

Cervone, G., Kafatos, M., Napoletani, D., & Singh, R.P.: Wavelet maxima curves of surface latent heat flux associated with two recent Greek earthquakes. Natural Hazards and Earth System Sciences 4(3): 359–374. doi:10.5194/nhess-4-359-2004, 2004.

Cervone, G., Maekawa, S., Singh, R.P., Hayakawa, M., Kafatos, M., & Shvets, A.: Surface latent heat flux and nighttime LF anomalies prior to the Mw = 8.3 TokachiOki earthquake. Natural Hazards and Earth System Sciences 6(1): 109–114. doi:10.5194/nhess-6-109-2006, 2006.

Cutler, D. R., Edwards, Jr. TC., Beard, K. H., Cutler, A., Hess, K. T., Gibson, J., & Lawler, J. J.: Random forests for classification in ecology. Ecology,88(11): 2783-2792, 2007.

Dey, S., & Singh, R.P.: Surface latent heat flux as an earthquake precursor. Natural Hazards and Earth System Sciences 3(6): 749–755. doi:10.5194/nhess-3-749-2003, 2003.

Dobrovolsky, I. R., Zubkov, S. I., & Myachkin, V. I.: Estimationof the size of earthquake preparation zones. Pure Appl. Geophys. (117): 1025–1044, 1979.

Dziak, R. P., Chadwick, W.W., Fox, C.G., & Embley, R.W.: Hydrothermal temperature changes at the southern Juan de Fuca Ridge associated with MW 6.2 Blanco Transform earthquake. Geology 31(2): 119–122. doi:10.1130/0091-7613(2003)031<0119:HTCATS>2.0.CO;2, 2003.

https://doi.org/10.5194/angeo-2021-41
Preprint. Discussion started: 1 September 2021




Eleftheriou, A., Filizzola, C., Genzano, N., Lacava, T., Lisi, M., Paciello, R., Pergola, N.,Vallianatos, F., & Tramutoli, V.: Longterm RST analysis of anomalous TIR sequences in relation with earthquakes occurred in Greece in the period 2004–2013. Pure and Applied Geophysics 173(1): 285-303. doi:10.1007/s00024-015-1116-8, 2016.

Freund, F. T., Kulahci, I.G., Cyr, G., Ling, J., Winnick, M., Tregloan-Reed, J., & Freund, M.M.: Air ionization at rock surfaces and pre-earthquake signals. Journal of Atmospheric and Solar-Terrestrial Physics 71(17): 1824–1834. doi:10.1016/j.jastp.2009.07.013, 2009.

Ganguly, N. D.: Variation in atmospheric ozone concentration following strong earthquakes. International Journal of Remote Sensing 30(2): 349–356. doi:10.1080/01431160802282862, 2009.

Ganguly, N. D.: Atmospheric changes observed during April 2015 Nepal earthquake. Journal of Atmospheric and Solar-Terrestrial Physics 140: 16–22. doi:10.1016/j.jastp.2016.01.017, 2016.

Ibanga, J.I., Akpan, A.E., George, N.J., Ekanem, A.M., & George, A.M.: Unusual ionospheric variations before the strong Auckland Islands, New Zealand earthquake of 30th September, 2007. NRIAG Journal of Astronomy and Geophysics 7(1): 149–154. doi:10.1016/j.nrjag.2017.12.007, 2018.

Jiao, Z. H., Zhao, J., &Shan, X.: Pre-seismic anomalies from optical satellite observations: a review. Natural Hazards and Earth System Sciences 18(4): 1013–1036. doi:10.5194/nhess-18-1013-2018, 2018.

Khosravi, I., Jouybari-Moghaddam, Y., and Sarajian, M. R.: The comparison of NN, SVR, LSSVR and ANFIS at modeling meteorological and remotely sensed drought indices over the eastern district of Isfahan, Iran. Natural Hazards, 87(3), 1507-1522, 2017.

Lebreton, J. P., Stverak, S., Travnicek, P., Maksimovic, M., Klinge, D., Merikallio, S., Lagoutte, D., Poirier, B., Blelly, P.L., Kozacek, Z., & Salaquarda, M.: The ISL Langmuir Probe experiment and its data processing onboard DEMETER: scientific objectives, description and first results. Planetary and Space Science 54(5): 472–486. doi:10.1016/j.pss.2005.10.017, 2006.

Li, M., & Parrot, M.: Real time analysis of the ion density measured by the satellite DEMETER in relation with the seismic activity. Natural Hazards and Earth System Sciences 12(9): 2957–2963. doi:10.5194/nhess-12-2957-2012, 2012.

Li, M., & Parrot, M.: Statistical analysis of an ionospheric parameter as a base for earthquake prediction. Journal of geophysical research: Space physics 118(6): 3731–3739. doi:10.1002/jgra.50313, 2013.

Li, M., & Parrot, M.: Statistical analysis of the ionospheric ion density recorded by DEMETER in the epicenter areas of earthquakes as well as in their magnetically conjugate point areas. Advances in Space Research 61(3): 974–984. doi:10.1016/j.asr.2017.10.047, 2018.

Liaw, A., & Wiener, M.: Classification and regression by random Forest. R news, 2(3), 18-22, 2002.

Liu, J. Y., Chuo, Y.J., Shan, S.J., Tsai, Y.B., Chen, Y.L., Pulinet, S.A., & Yu, S.B.: Pre-earthquake ionospheric anomalies registered by continuous GPS TEC measurements. AnnalesGeophysicae 22(5): 1585–1593. doi:10.5194/angeo-22-1585-2004, 2004.

MansouriDaneshvar, M. R., Khosravi, M., & Tavousi, T.: Seismic triggering of atmospheric variables prior to the major earthquakes in the Middle East within a 12-year time-period of 2002–2013. Natural Hazards 74(3): 1539–1553. doi:10.1007/s11069-014-1266-5, 2014.

Panda, S. K., Choudhury, S., Saraf, A.K., & Das, J.D.: MODIS land surface temperature data detects thermal anomaly preceding 8 October 2005 Kashmir earthquake. International Journal of Remote Sensing 28(20): 4587–4596. doi:10.1080/01431160701244906, 2007.

Parrot, M., D. Benoist, Berthelier, J.J., Błęcki, J., Chapuis, Y., Colin, F., Elie, F., Fergeau, P., Lagoutte, D., Lefeuvre, F., Legendre, C., Lévêque, M., Pinçon, J.L., Poirier, B., Seran, H.C., & Zamora, P.: The magnetic field experiment IMSC and its data processing onboard DEMETER: scientific objectives, description and first results. Planetary and Space Science 54(5): 441–455. doi:10.1016/j.pss.2005.10.015, 2006.

https://doi.org/10.5194/angeo-2021-41
Preprint. Discussion started: 1 September 2021




Parrot, M., Tramutoli, V., Liu, T.J.Y., Pulinets, S., Ouzounov, D., Genzano, N., Lisi, M., Hattori, K., & Namgaladze, A.: Atmospheric and ionospheric coupling phenomena related to large earthquakes. Natural Hazards and Earth System Sciences. doi: 10.5194/nhess-2016-172, 2016.

Pulinets, S., & Ouzounov, D.: Lithosphere–Atmosphere– Ionosphere Coupling (LAIC) model – An unified concept for earthquake precursors validation. Journal of Asian Earth Sciences 41(4): 371-382. doi:10.1016/j.jseaes.2010.03.005, 2011.

Pulinets, S. A., Ouzounov, D., Ciraolo, L., Singh, R., Cervone, G., Leyva, A., Dunajecka, M., Karelin, A.Y., Boyarchuk, K.A., & Kotsarenko, A.: Thermal, atmospheric and ionospheric anomalies around the time of the Colima M7.8 earthquake of 21 January 2003. AnnalesGeophysicae 24(3): 835–849. doi:10.5194/angeo-24-835-2006 , 2006.

Ouzounov, D., & Freund, F.: Mid-infrared emission prior to strong earthquakes analyzed by remote sensing data. Advances in Space Research 33(3): 268–273. doi:10.1016/S0273-1177(03)00486-1, 2004.

Ouzounov, D., Bryant, N., Logan, T., Pulinets, S., & Taylor, P.: Satellite thermal IR phenomena associated with some of the major earthquakes in 1999–2003. Physics and Chemistry of the Earth, Parts A/B/C 31(4): 154–163. doi:10.1016/j.pce.2006.02.036, 2006.

Ouzounov, D., Liu, D., Chunli, K., Cervone, G., Kafatos, M., & Taylor, P.: Outgoing long wave radiation variability from IR satellite data prior to major earthquakes. Tectonophysics 431(1): 211–220. doi:10.1016/j.tecto.2006.05.042, 2007.

Qin, K., Wu, L.X., Ouyang, X.Y., Shen, X.H., & Zheng, S.: Surface latent heat flux anomalies quasi-synchronous with ionospheric disturbances before the 2007 Pu'er earthquake in China. Advances in Space Research 53(2): 266–271. doi:10.1016/j.asr.2013.11.004, 2014.

Rawat, V., Saraf, A.K., Das, J., Sharma, K., & Shujat, Y.: Anomalous land surface temperature and outgoing long-wave radiation observations prior to earthquakes in India and Romania. Natural Hazards 59(1): 33–46. doi:10.1007/s11069-011-9736-5, 2011.

Saradjian, M.R., andAkhoondzadeh, M.: Prediction of the date, magnitude and affected area of impending strong earthquakes using integration of multi precursors earthquake parameters. Natural Hazards and Earth System Sciences 11(4): 1109–1119. doi:10.5194/nhess-11-1109-2011, 2011.

Saraf, A.K., Rawat, V., Banerjee, P., Choudhury, S., Panda, S.K., Dasgupta, S., & Das, J.D.: Satellite detection of earthquake thermal infrared precursors in Iran. Natural Hazards 47(1): 119–135. doi:10.1007/s11069-007-9201-7, 2008.

Schaer, S., Gurtner, W., &Feltens, J.: IONEX: the IONosphere map EXchange format version 1. In: Proceedings of the 1988 IGS Analysis Centers Workshop. ESOC, Darmstadt, Germany, 233-247. February 9-11, 1998.

Tao, D., Cao, J., Battiston, R., Li, L., Ma, Y., Lie, W., Zima, Z., Wand, L., & Dunlop, M.W.: Seismo-ionospheric anomalies in ionospheric TEC and plasma density before the 17 July 2006 M7.7 south of Java earthquake. AnnalesGeophysicae 35(3): 589–598. doi:10.5194/angeo-35-589-2017, 2017

Tronin, A. A.: Remote sensing and earthquakes: A review. Physics and Chemistry of the Earth, Parts A/B/C 31(4): 138–142. doi:10.1016/j.pce.2006.02.024, 2006.

Wackerly, D., Mendenhall, W., Scheaffer, R.L., "Mathematical Statistics with Applications (7 ed.)." Belmont, CA, USA: Thomson Higher Education, 2008.

Wan, Z.: New refinements and validation of the collection-6 MODIS land-surface temperature/emissivity product. Remote Sensing of Environment 140: 36–45. doi:10.1016/j.rse.2013.08.027, 2014

Zhang, W., Zhao, J., Wang, W., Ren, H., Chen, L., &Yan, G.: A preliminary evaluation of surface latent heat flux as an earthquake precursor. Natural Hazards and Earth System Sciences 13(10): 2639–2647. doi:10.5194/nhess-13-2639-2013, 2013, 2013.

Zoran, M.: MODIS and NOAA-AVHRR l and surface temperature data detect a thermal anomaly preceding the 11 March 2011 Tohoku earthquake. International Journal of Remote Sensing 33(21): 6805–6817, doi:10.1080/01431161.2012.692833, 2012.

https://doi.org/10.5194/angeo-2021-41
Preprint. Discussion started: 1 September 2021


Annales Geophysicae Discussions

**Table 1. Earthquake magnitude estimation (Saradjian and Akhoondzadeh 2011)**

| $D_x$ value | Earthquake magnitude |
|---|---|
| $D_x \leq 1$ | $Mw \leq 6$ |
| $1 < D_x \leq 2$ | $6 < Mw \leq 7$ |
| $2 < D_x \leq 3$ | $7 < Mw \leq 8$ |
| $3 < D_x$ | $8 < Mw$ |

**Table 2. Characteristics of earthquakes investigated in this study (http://earthquake.usgs.gov/)**

| Case Study | Date | Time (UTC) | Latitude | Longitude | Mw | Depth (km) |
|---|---|---|---|---|---|---|
| Kermanshah, Iran | 2017-11-12 | 18:18:17 | 34.91 E | 45.96 N | 7.3 | 19 |
| Samoa Islands | 2009-09-29 | 17:48:10 | 15.59 W | 172.10 S | 8.1 | 18 |
| Sichuan, China | 2008-05-12 | 06:28:01 | 31.00 E | 103.32 N | 7.9 | 19 |
| Bam, Iran | 2003-12-26 | 01:56:52 | 29.00 E | 58.31 N | 6.6 | 10 |

**Table 3. List of anomalies obtained from different precursors of Kermanshah earthquake using Median method**

| Precursor | Date of observed anomaly | Prediction of earthquake date | Deviation value (Dx) | Prediction of earthquake magnitude (Mw) |
|---|---|---|---|---|
| TEC | 4 Nov (UTC=04:00) | 5 Nov-19 Nov | 2.23 | 7<Mw<8 |
| | 3 Nov (UTC=22:00) | 4 Nov-18 Nov | 2.11 | 7<Mw<8 |
| | 3 Nov (UTC=20:00) | 4 Nov-18 Nov | 2.42 | 7<Mw<8 |
| | 3 Nov (UTC=18:00) | 4 Nov-18 Nov | 2.31 | 7<Mw<8 |
| | 3 Nov (UTC=12:00) | 4 Nov-18 Nov | 2.43 | 7<Mw<8 |
| LST Terra (Day Time) | 19 oct | 20 oct-4 Nov | -3.2 | Mw>8 |
| Aerosol Optical Depth (OMI) | 26 Oct | 27 Oct-10 Nov | 9.42 | Mw>8 |
| Aerosol Optical Depth (Aqua) | 31 Oct | 1 Nov-15 Nov | 3.96 | Mw>8 |
| Aerosol Optical Depth (Terra) | 31 Oct | 1 Nov-15 Nov | 3.55 | Mw>8 |
| SLHF | 6 Nov | 7 Nov-22 Nov | 7.77 | Mw>8 |
| | 5 Nov | 6 Nov-21 Nov | 4.35 | Mw>8 |
| | 3 Nov | 4 Nov-19 Nov | 8.93 | Mw>8 |

**Table 4. List of anomalies obtained from different precursors of Kermanshah earthquake using SVR method**

| Precursor | Date of observed anomaly | Prediction of earthquake date | Deviation value (Dx) | Prediction of earthquake magnitude (Mw) |
|---|---|---|---|---|
| TEC | 4 Nov (UTC=04:00) | 5 Nov-19 Nov | 2.22 | 7<Mw<8 |
| | 3 Nov (UTC=12:00) | 4 Nov-18 Nov | 2.73 | 7<Mw<8 |
| | 3 Nov (UTC=18:00) | 4 Nov-18 Nov | 2.56 | 7<Mw<8 |
| | 3 Nov (UTC=20:00) | 4 Nov-18 Nov | 2.43 | 7<Mw<8 |
| | 3 Nov (UTC=22:00) | 4 Nov-18 Nov | 2.09 | 7<Mw<8 |
| Aerosol Optical Depth (OMI) | 26 Oct | 27 Oct-10 Nov | 4.07 | Mw>8 |
| Aerosol Optical Depth (Aqua) | 31 Oct | 1 Nov-15 Nov | 3.02 | Mw>8 |
| Aerosol Optical Depth (Terra) | 2 Nov | 3 Nov-17 Nov | 2.53 | 7<Mw<8 |
| | 31 Oct | 1 Nov-15 Nov | 2.81 | 7<Mw<8 |
| SLHF | 6 Nov | 7 Nov-22 Nov | 6.30 | Mw>8 |
| | 5 Nov | 6 Nov-21 Nov | 3.66 | Mw>8 |
| | 3 Nov | 4 Nov-19 Nov | 7.15 | Mw>8 |

**Table 5. List of anomalies obtained from different precursors of Kermanshah earthquake using Random Forest method**

| Precursor | Date of observed anomaly | Prediction of earthquake date | Deviation value (Dx) | Prediction of earthquake magnitude (Mw) |
|---|---|---|---|---|
| TEC | 4 Nov (UTC=04:00) | 5 Nov-19 Nov | 2.22 | 7<Mw<8 |

https://doi.org/10.5194/angeo-2021-41
Preprint. Discussion started: 1 September 2021


Annales Geophysicae Discussions
Open Access
EGU

| | | | | |
|---|---|---|---|---|
| | 3 Nov (UTC=20:00) | 4 Nov-18 Nov | 2.35 | 7<Mw<8 |
| | 3 Nov (UTC=12:00) | 4 Nov-18 Nov | 2.27 | 7<Mw<8 |
| | 3 Nov (UTC=22:00) | 4 Nov-18 Nov | 2.16 | 7<Mw<8 |
| | 3 Nov (UTC=18:00) | 4 Nov-18 Nov | 2.10 | 7<Mw<8 |
| LST Terra (Day Time) | 19 Oct | 20 Oct-4 Nov | -2.02 | 7<Mw<8 |
| Aerosol Optical Depth (OMI) | 2 Nov | 3 Nov-17 Nov | 3.25 | Mw>8 |
| | 31 Oct | 1 Nov-15 Nov | 3.86 | Mw>8 |
| | 26 Oct | 27 Oct-10 Nov | 19.70 | Mw>8 |
| Aerosol Optical Depth (Aqua) | 31 Oct | 1 Nov-15 Nov | 2.69 | 7<Mw<8 |
| Aerosol Optical Depth (Terra) | 2 Nov | 3 Nov-17 Nov | 2.17 | 7<Mw<8 |
| | 31 Oct | 1 Nov-15 Nov | 3.60 | Mw>8 |
| SLHF | 6 Nov | 7 Nov-22 Nov | 7.81 | Mw>8 |
| | 5 Nov | 6 Nov-21 Nov | 4.35 | Mw>8 |
| | 3 Nov | 4 Nov-19 Nov | 8.95 | Mw>8 |

**Table 6. List of anomalies obtained from different precursors of the Samoa Earthquake using Median method**

| Precursor | Date of observed anomaly | Prediction of earthquake date | Deviation value (Dx) | Prediction of earthquake magnitude (Mw) |
|---|---|---|---|---|
| Total Ion Density (DayTime) | 25 Sep | 26 Sep-10 Oct | 4.19 | Mw>8 |
| Electron Density (DayTime) | 25 Sep | 26 Sep-10 Oct | 2.79 | 7<Mw<8 |
| Ion Density (DayTime) | 25 Sep | 26 Sep-10 Oct | 2.66 | 7<Mw<8 |
| Total Ion Density (Night Time) | 24 Sep | 25 Sep-9 Oct | 2.50 | 7<Mw<8 |
| Electron Density (NightTime) | 24 Sep | 25 Sep-9 Oct | 2.67 | 7<Mw<8 |
| Ion Density (Night Time) | 24 Sep | 25 Sep-9 Oct | 2.92 | 7<Mw<8 |
| Total Ion Density (NightTime) | 5 Sep | 6 Sep-20 Oct | 2.02 | 7<Mw<8 |
| Electron Density (DayTime) | 5 Sep | 6 Sep-20 Oct | 2.28 | 7<Mw<8 |
| Ion Density (DayTime) | 5 Sep | 6 Sep-20 Oct | 2.32 | 7<Mw<8 |
| TEC | 28 Sep (UTC=14:00) | 29 Sep-13 Oct | 2.26 | 7<Mw<8 |
| | 25 Sep (UTC=24:00) | 26 Sep-10 Oct | 2.7 | 7<Mw<8 |
| | 25 Sep (UTC=18:00) | 26 Sep-10 Oct | -2.21 | 7<Mw<8 |
| | 18 Sep (UTC=08:00) | 19 Sep-3 Oct | 2.59 | 7<Mw<8 |
| Sea Surface Temperature | 7 Sep | 8 Sep-23 Sep | 3.31 | Mw>8 |
| | 6 Sep | 7 Sep-22 Sep | 4.72 | Mw>8 |
| Aerosol Optical Depth (OMI) | 19 Sep | 20 Sep-4 Oct | 2.56 | 7<Mw<8 |
| Aerosol Optical Depth (Terra) | 21 Sep | 22 Sep-6 Oct | 2.08 | 7<Mw<8 |
| | 30 Aug | 31 Aug-14 Sep | 2.07 | 7<Mw<8 |

440

**Table 7. List of anomalies obtained from different precursors of the Samoa earthquake using SVR method**

| Precursor | Date of observed anomaly | Prediction of earthquake date | Deviation value (Dx) | Prediction of earthquake magnitude (Mw) |
|---|---|---|---|---|
| Total Ion Density (DayTime) | 25 Sep | 26 Sep-10 Oct | 4.37 | Mw>8 |
| Electron Density (DayTime) | 25 Sep | 26 Sep-10 Oct | 2.29 | 7<Mw<8 |
| Ion Density (DayTime) | 25 Sep | 26 Sep-10 Oct | 2.20 | 7<Mw<8 |
| Electron Density (NightTime) | 24 Sep | 25 Sep-9 Oct | 2.74 | 7<Mw<8 |
| TEC | 28 Sep (UTC=14:00) | 29 Sep-13 Oct | 2.45 | 7<Mw<8 |
| | 27 Sep (UTC=18:00) | 28 Sep-12 Oct | 2.28 | 7<Mw<8 |
| Sea Surface Temperature | 9 Sep | 10 Sep-25 Sep | -3.51 | Mw>8 |
| | 7 Sep | 8 Sep-23 Sep | 3.36 | Mw>8 |
| | 6 Sep | 7 Sep-22 Sep | 4.47 | Mw>8 |
| Aerosol Optical Depth (OMI) | 19 Sep | 20 Sep-4 Oct | 3.21 | Mw>8 |

**Table 8. List of anomalies obtained from different precursors of the Samoa earthquake using Random Forest method**

| Precursor | Date of observed anomaly | Prediction of earthquake date | Deviation value (Dx) | Prediction of earthquake magnitude (Mw) |
|---|---|---|---|---|
| Total Ion Density (DayTime) | 25 Sep | 26 Sep-10 Oct | 4.42 | Mw>8 |
| Electron Density (DayTime) | 25 Sep | 26 Sep-10 Oct | 2.74 | 7<Mw<8 |
| Ion Density (DayTime) | 25 Sep | 26 Sep-10 Oct | 2.53 | 7<Mw<8 |
| Ion Density (Night Time) | 24 Sep | 25 Sep-9 Oct | 2.78 | 7<Mw<8 |
| Electron Density (NightTime) | 24 Sep | 25 Sep-9 Oct | 2.16 | 7<Mw<8 |
| Total Ion Density (DayTime) | 21 Sep | 22 Sep-6 Oct | 2.05 | 7<Mw<8 |
| Ion Density (DayTime) | 5 Sep | 6 Sep-20 Oct | 2.05 | 7<Mw<8 |

https://doi.org/10.5194/angeo-2021-41
Preprint. Discussion started: 1 September 2021




| | | | | |
|---|---|---|---|---|
| Electron Density (DayTime) | 5 Sep | 6 Sep-20 Oct | 2.02 | 7<Mw<8 |
| TEC | 28 Sep (UTC=14:00) | 29 Sep-13 Oct | 2.43 | 7<Mw<8 |
| | 27 Sep (UTC=14:00) | 28 Sep-12 Oct | 2.7 | 7<Mw<8 |
| | 25 Sep (UTC=16:00) | 26 Sep-10 Oct | -2.21 | 7<Mw<8 |
| Sea Surface Temperature | 18 Sep | 19 Sep-4 Oct | 2.22 | 7<Mw<8 |
| | 7 Sep | 8 Sep-23 Sep | 5.55 | Mw>8 |
| | 6 Sep | 7 Sep-22 Sep | 4.07 | Mw>8 |
| Aerosol Optical Depth (OMI) | 19 Sep | 20 Sep-4 Oct | 3.21 | Mw>8 |
| Aerosol Optical Depth (Terra) | 12 Sep | 13 Sep-27 Sep | 2.04 | 7<Mw<8 |

**Table 9. List of anomalies obtained from different precursors of the Sichuan Earthquake using Median method**

| Precursor | Date of observed anomaly | Prediction of earthquake date | Deviation value (Dx) | Prediction of earthquake magnitude (Mw) |
|---|---|---|---|---|
| Ion Temperature (Night Time) | 9 May | 10 May-24 May | 2.92 | 7<Mw<8 |
| Electron Density (Day Time) | 21 Apr | 22 Apr-6 May | 2.73 | 7<Mw<8 |
| Ion Density (Day Time) | 21 Apr | 22 Apr-6 May | 2.68 | 7<Mw<8 |
| Total Ion Density (DayTime) | 21 Apr | 22 Apr-6 May | 2.37 | 7<Mw<8 |
| TEC | 9 May(UTC=10:00) | 10 May-24 May | 2.86 | 7<Mw<8 |
| | 9 May (UTC=14:00) | 10 May-24 May | -2.67 | 7<Mw<8 |
| | 3 May (UTC=06:00) | 4 May-18 May | 2.63 | 7<Mw<8 |
| | 3 May (UTC=18:00) | 4 May-18 May | 2.31 | 7<Mw<8 |
| | 21 Apr (UTC=06:00) | 22 Apr-6 May | 2.53 | 7<Mw<8 |
| LST Aqua (NightTime) | 3 May | 4 May-19 May | -3.5 | Mw>8 |
| LST Aqua (Day Time) | 21 Apr | 22 Apr-7 May | -4.10 | Mw>8 |
| Aerosol Optical Depth (OMI) | 21 Apr | 22 Apr-6 May | 7.33 | Mw>8 |
| Aerosol Optical Depth (Aqua) | 9 May | 10 May-24 May | 2.25 | 7<Mw<8 |
| SLHF | 25 Apr | 26 Apr-12 May | 2.14 | 7<Mw<8 |

**Table 10. List of anomalies obtained from different precursors of the Sichuan Earthquake using SVR method**

| Precursor | Date of observed anomaly | Prediction of earthquake date | Deviation value (Dx) | Prediction of earthquake magnitude(Mw) |
|---|---|---|---|---|
| Ion Temperature (Night Time) | 9 May | 10 May-24 May | 3 | Mw>8 |
| Ion Density (Day Time) | 21 Apr | 22 Apr-6 May | 2.69 | 7<Mw<8 |
| Electron Density (Day Time) | 21 Apr | 22 Apr-6 May | 2.52 | 7<Mw<8 |
| Total Ion Density (DayTime) | 21 Apr | 22 Apr-6 May | 2.11 | 7<Mw<8 |
| TEC | 9 May(UTC=10:00) | 10 May-24 May | 3.92 | Mw>8 |
| | 3 May(UTC=04:00) | 4 May-18 May | 2.73 | 7<Mw<8 |
| | 3 May (UTC=18:00) | 4 May-18 May | 2.50 | 7<Mw<8 |
| | 21 Apr (UTC=04:00) | 22 Apr-6 May | 3.09 | Mw>8 |
| | 18 Apr (UTC=10:00) | 19 Apr-3 May | 2.50 | 7<Mw<8 |
| LST Aqua (NightTime) | 3 May | 4 May-19 May | -2.37 | 7<Mw<8 |
| LST Aqua (Day Time) | 21 Apr | 22 Apr-7 May | -4.08 | Mw>8 |
| Aerosol Optical Depth (OMI) | 21 Apr | 22 Apr-6 May | 5.38 | Mw>8 |
| Aerosol Optical Depth (Aqua) | 9 May | 10 May-24 May | 2.32 | 7<Mw<8 |

**Table 11. List of anomalies obtained from different precursors of the Sichuan Earthquake using Random Forest method**

| Precursor | Date of observed anomaly | Prediction of earthquake date | Deviation value (Dx) | Prediction of earthquake magnitude (Mw) |
|---|---|---|---|---|
| Ion Temperature (Night Time) | 9 May | 10 May-24 May | 2.80 | 7<Mw<8 |
| Ion Density (Day Time) | 28 Apr | 29 Apr-13 May | 2.09 | 7<Mw<8 |
| Ion Density (Day Time) | 21 Apr | 22 Apr-6 May | 2.85 | 7<Mw<8 |
| Electron Density (DayTime) | 21 Apr | 22 Apr-6 May | 2.83 | 7<Mw<8 |
| TEC | 9 May(UTC=10:00) | 10 May-24 May | 3.40 | Mw>8 |
| | 3 May (UTC=04:00) | 4 May-18 May | 2.56 | 7<Mw<8 |
| | 3 May (UTC=18:00) | 4 May-18 May | 2.39 | 7<Mw<8 |
| | 21 Apr (UTC=04:00) | 22 Apr-6 May | 3.18 | Mw>8 |
| | 21 Apr (UTC=06:00) | 22 Apr-6 May | 2.32 | 7<Mw<8 |
| LST Aqua (NightTime) | 3 May | 4 May-19 May | -3.41 | Mw>8 |
| LST Aqua (Day Time) | 21 Apr | 22 Apr-7 May | -3.71 | Mw>8 |
| Aerosol Optical Depth (OMI) | 21 Apr | 22 Apr-6 May | 5.62 | Mw>8 |

https://doi.org/10.5194/angeo-2021-41
Preprint. Discussion started: 1 September 2021


Annales Geophysicae Discussions
Open Access
EGU

**Table 12. List of anomalies obtained from different precursors of Bam Earthquake using Median method**

| Precursor | Date of observed anomaly | Prediction of earthquake date | Deviation value (Dx) | Prediction of earthquake magnitude (Mw) |
|---|---|---|---|---|
| TEC | 19 Dec (UTC=24:00) | 20 Dec-3 Jan | 1.14 | 6<Mw<7 |
| | 17 Dec (UTC=12:00) | 18 Dec-1 Jan | 1.04 | 6<Mw<7 |
| | 16 Dec (UTC=02:00) | 17 Dec-31 Dec | -1.26 | 6<Mw<7 |
| LST Aqua (NightTime) | 14 Dec | 15 Dec-30 Dec | -1.68 | 6<Mw<7 |
| LST Aqua (Day Time) | 13 Dec | 14 Dec-29 Dec | -2.32 | 7<Mw<8 |
| LST Aqua (NightTime) | 13 Dec | 14 Dec-29 Dec | -1.87 | 6<Mw<7 |
| LST Terra (Day Time) | 13 Dec | 14 Dec-29 Dec | -1.77 | 6<Mw<7 |
| LST Aqua (Day Time) | 12 Dec | 13 Dec-28 Dec | -2.91 | 7<Mw<8 |
| LST Terra (Day Time) | 12 Dec | 13 Dec-28 Dec | -2.02 | 7<Mw<8 |
| LST Terra(NightTime) | 12 Dec | 13 Dec-28 Dec | -1.81 | 6<Mw<7 |
| LST Terra(NightTime) | 7 Dec | 8 Dec-23 Dec | 1.91 | 6<Mw<7 |
| LST Aqua (NightTime) | 7 Dec | 8 Dec-23 Dec | 1.83 | 6<Mw<7 |
| LST Terra (NightTime) | 6 Dec | 7 Dec-22 Dec | 2.14 | 7<Mw<8 |
| LST Terra (Day Time) | 30 Nov | 1 Dec-16 Dec | -3.32 | Mw>8 |
| Aerosol Optical Depth (Aqua) | 12 Dec | 13 Dec-27 Dec | 4.51 | Mw>8 |
| Aerosol Optical Depth (Terra) | 12 Dec | 13 Dec-27 Dec | 3.42 | Mw>8 |
| | 13 Nov | 14 Nov-28 Dec | 2.29 | 7<Mw<8 |
| SLHF | 24 Dec | 25 Dec-9 Jan | 2.53 | 7<Mw<8 |
| | 16 Dec | 17 Dec-1 Jan | 4.52 | Mw>8 |
| | 15 Dec | 16 Dec-31 Dec | 8.12 | Mw>8 |
| | 29 Nov | 30 Nov-15 Dec | 6.23 | Mw>8 |
| | 28 Nov | 29 Nov-14 Dec | 3.14 | Mw>8 |

**Table 13. List of anomalies obtained from different precursors of the Bam earthquake using SVR method**

| Precursor | Date of observed anomaly | Prediction of earthquake date | Deviation value (Dx) | Prediction of earthquake magnitude (Mw) |
|---|---|---|---|---|
| TEC | 19 Dec (UTC=12:00) | 20 Dec-3 Jan | -1.18 | 6<Mw<7 |
| | 18 Dec (UTC=10:00) | 19 Dec-2 Jan | 1.08 | 6<Mw<7 |
| | 17 Dec (UTC=18:00) | 17 Dec-31 Dec | 2.65 | 7<Mw<8 |
| | 17 Dec (UTC=16:00) | 17 Dec-31 Dec | 1.61 | 6<Mw<7 |
| LST Aqua (Night Time) | 18 Dec | 19 Dec-3 Jan | -1.66 | 6<Mw<7 |
| LST Aqua (Day Time) | 13 Dec | 14 Dec-29 Dec | -2.67 | 7<Mw<8 |
| LST Aqua (Day Time) | 12 Dec | 13 Dec-28 Dec | -3.43 | Mw>8 |
| LST Terra (NightTime) | 12 Dec | 13 Dec-28 Dec | -2.10 | 7<Mw<8 |
| LST Terra(DayTime) | 12 Dec | 13 Dec-28 Dec | -1.74 | 7<Mw<8 |
| LST Terra(NightTime) | 5 Dec | 6 Dec-21 Dec | 2.33 | 7<Mw<8 |
| LST Terra (NightTime) | 3 Dec | 4 Dec-19 Dec | -2.36 | 7<Mw<8 |
| Aerosol Optical Depth (Aqua) | 12 Dec | 13 Dec-27 Dec | 3.70 | Mw>8 |
| Aerosol Optical Depth (Terra) | 14 Dec | 15 Dec-29 Dec | -3.09 | Mw>8 |
| | 13 Dec | 14 Dec-28 Dec | 2.04 | 7<Mw<8 |
| | 12 Dec | 13 Dec-27 Dec | 4.37 | Mw>8 |
| SLHF | 24 Dec | 25 Dec-9 Jan | 2.25 | 7<Mw<8 |
| | 16 Dec | 17 Dec-1 Jan | 4.08 | Mw>8 |
| | 15 Dec | 16 Dec-31 Dec | 6.77 | Mw>8 |

**Table 14. List of anomalies obtained from different precursors of Bam Earthquake using Random Forest method**

| Precursor | Date of observed anomaly | Prediction of earthquake date | Deviation value (Dx) | Prediction of earthquake magnitude (Mw) |
|---|---|---|---|---|
| TEC | 19 Dec (UTC=24:00) | 20 Dec-3 Jan | 1.20 | 6<Mw<7 |
| | 18 Dec (UTC=10:00) | 19 Dec-2 Jan | 1.29 | 6<Mw<7 |
| | 17 Dec (UTC=16:00) | 18 Dec-1 Jan | 3.04 | Mw>8 |
| | 17 Dec (UTC=18:00) | 18 Dec-1 Jan | 2.17 | 7<Mw<8 |
| LST Aqua (NightTime) | 18 Dec | 19 Dec-3 Jan | -2.02 | 7<Mw<8 |
| LST Aqua (DayTime) | 13 Dec | 14 Dec-29 Dec | -2.97 | 6<Mw<7 |
| LST Aqua (Day Time) | 12 Dec | 13 Dec-28 Dec | -4.00 | 7<Mw<8 |
| LST Terra (DayTime) | 12 Dec | 13 Dec-28 Dec | -1.67 | 6<Mw<7 |
| LST Aqua (Night Time) | 7 Dec | 8 Dec-23 Dec | 1.61 | 6<Mw<7 |
| Aerosol Optical Depth (Aqua) | 12 Dec | 13 Dec-27 Dec | 4.99 | Mw>8 |
| Aerosol Optical Depth (Terra) | 12 Dec | 13 Dec-27 Dec | 3.99 | Mw>8 |
| SLHF | 24 Dec | 25 Dec-9 Jan | 2.50 | 7<Mw<8 |

https://doi.org/10.5194/angeo-2021-41
Preprint. Discussion started: 1 September 2021


Annales Geophysicae Discussions
Open Access
EGU

| | | | | |
|---|---|---|---|---|
| | 16 Dec | 17 Dec-1 Jan | 4.32 | Mw>8 |
| | 15 Dec | 16 Dec-31 Dec | 7.49 | Mw>8 |

**Table 15. The registered and estimated earthquake parameters related to the case studies**

| Case Study | Earthquake Date | | | | Earthquake Magnitude ($M_w$) | | | |
|---|---|---|---|---|---|---|---|---|
| | Registered | Estimated MSE Method | | | Registered | Estimated MSE Method | | |
| | | Median | SVR | RF | | Median | SVR | RF |
| Kermanshah | 12 Nov 2017 | 4-19 Nov 2017 | 4-18 Nov 2017 | 4-18 Nov 2017 | 7.3 | >8 | 7-8 | 7-8 |
| Samoa | 29 Sep 2009 | 25 Sep-9 Oct 2009 | 24 Sep-9 Oct 2009 | 25 Sep-9 Oct 2009 | 8.1 | 7-8 | 7-8 | 7-8 |
| Sichuan | 12 May 2008 | 4-18 May 2008 | 5-19 May 2008 | 7-21 May 2008 | 7.9 | 7-8 | 7-8 | 7-8 |
| Bam | 26 Dec 2003 | 13-28 Dec 2003 | 16-31 Dec 2003 | 16-30 Dec 2003 | 6.6 | 7-8 | 6-7 | 7-8 |

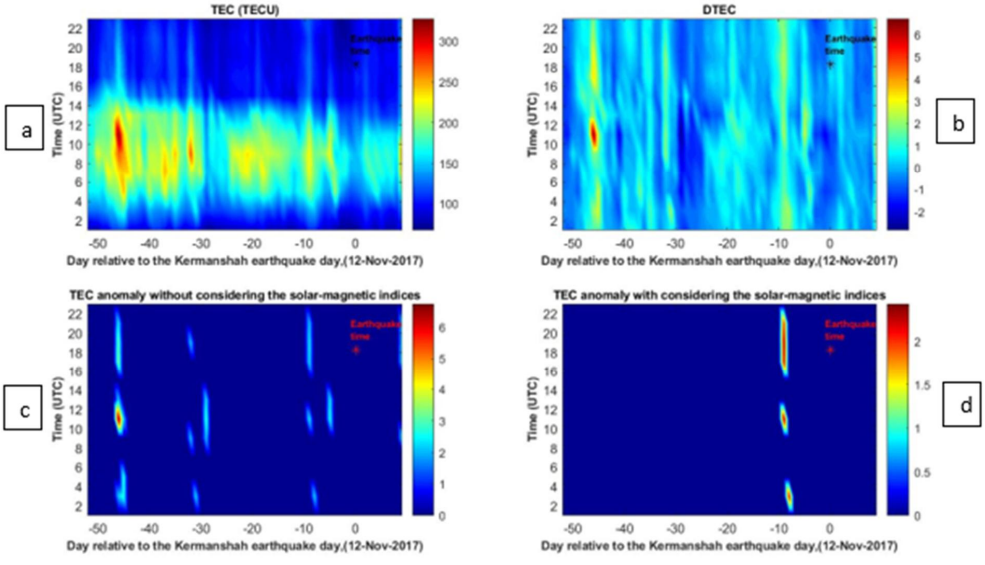


**Fig. 1. Results of TEC Analysis using median for Kermanshah earthquake. The earthquake time is indicated by an asterisk. (a) TEC variations, (b) DTEC, (c) Detected anomalies without considering the solar-magnetic indices, (d) Detected anomalies with considering the solar-magnetic indices.**

https://doi.org/10.5194/angeo-2021-41
Preprint. Discussion started: 1 September 2021


Annales Geophysicae Discussions
Open Access
EGU

470

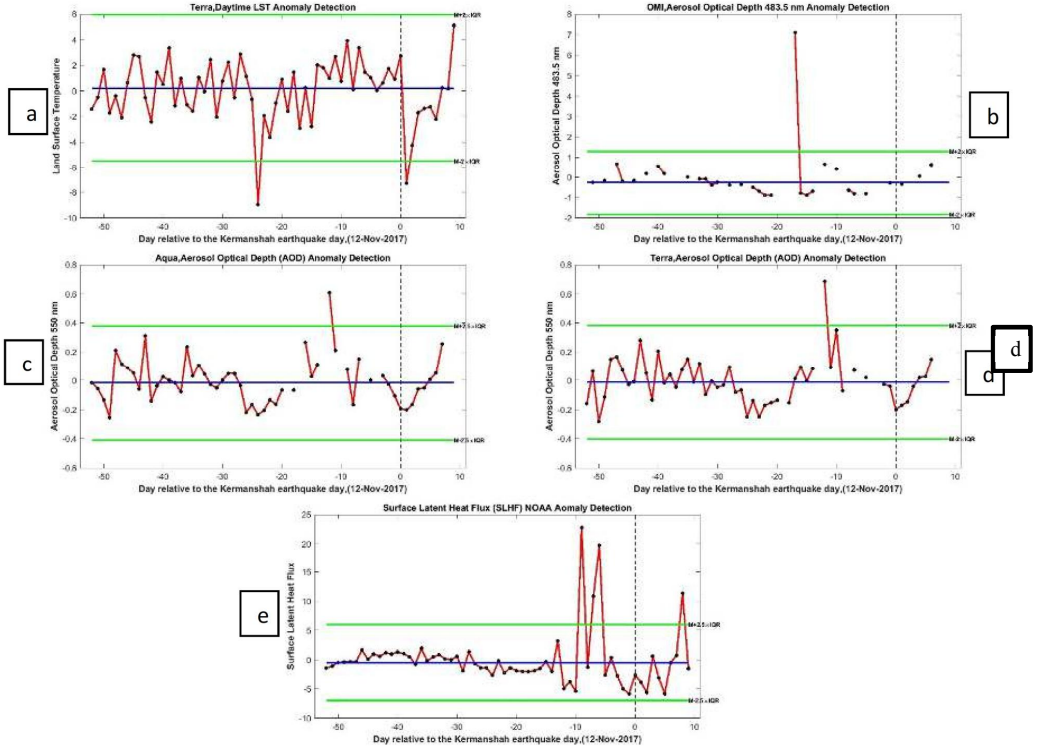


**Fig. 2. Results of (a) Daytime LST data (Terra, MODIS), (b) AOD data (OMI), (c) AOD (Aqua, MODIS), (d) AOD (Terra, MODIS), (e) SLHF (NOAA), analysis using median method for Kermanshah earthquake. The earthquake day is displayed as a vertical dotted line. The green horizontal lines indicate the higher and lower bounds. The blue line indicates the median value.**

475

https://doi.org/10.5194/angeo-2021-41
Preprint. Discussion started: 1 September 2021


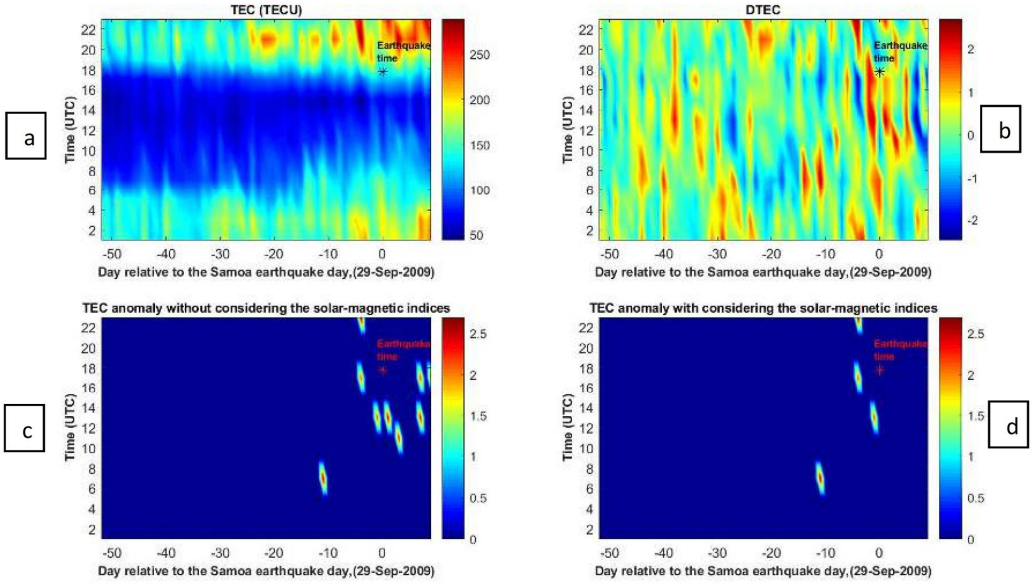


**Fig. 3. Results of TEC Analysis using median for Samoa earthquake. The earthquake time is indicated by an asterisk. (a) TEC variations, (b) DTEC, (c) Detected anomalies without considering the solar-magnetic indices, (d) Detected anomalies with considering the solar-magnetic indices.**

480

https://doi.org/10.5194/angeo-2021-41
Preprint. Discussion started: 1 September 2021


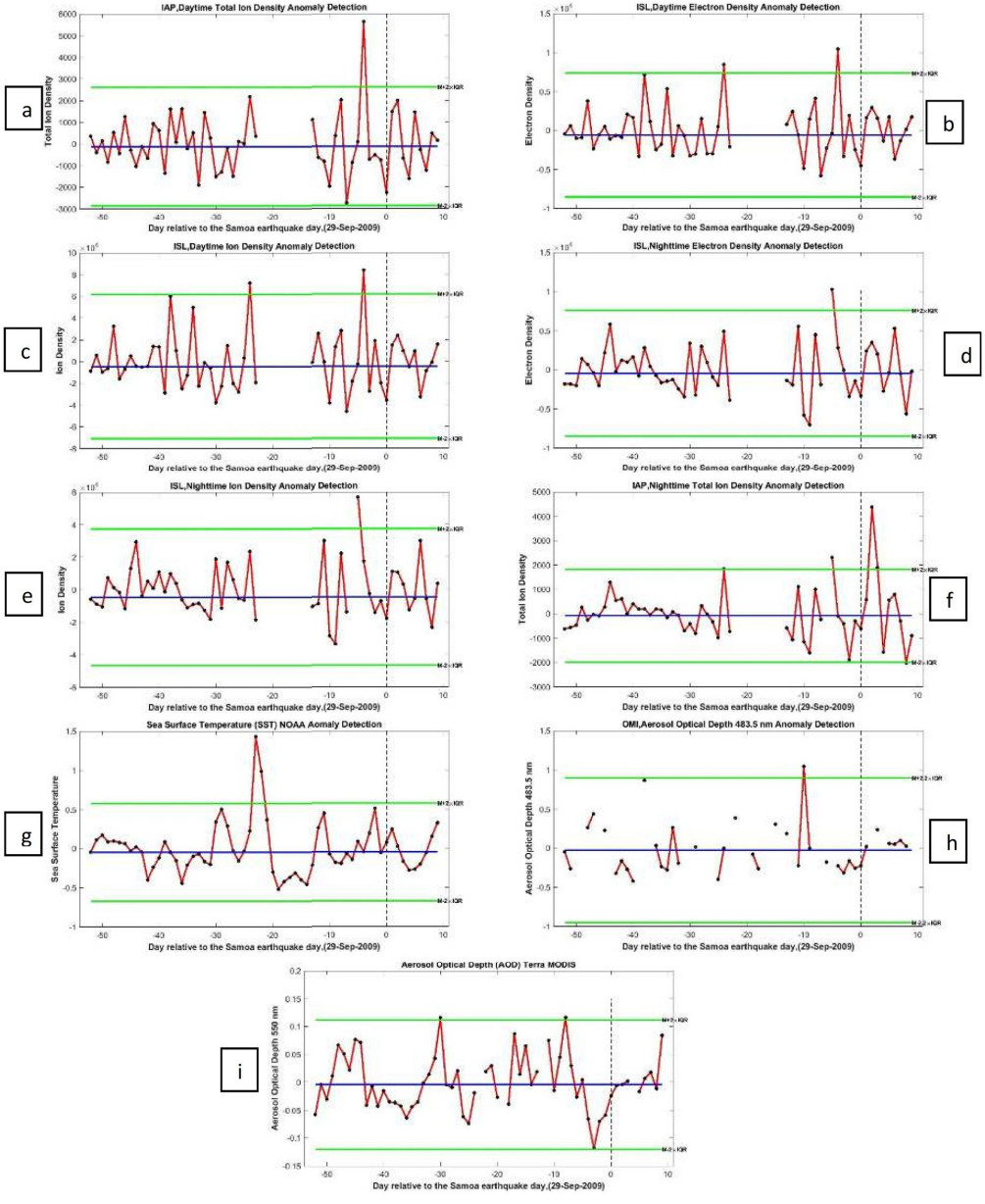


**Fig. 4. Results of (a) Daytime total ion density data (IAP, DEMETER), (b) Daytime electron density data (ISL, DEMETER), (c) Daytime ion density data (ISL, DEMETER), (d) Nighttime electron density data (ISL, DEMETER), (e) Nighttime ion density data (ISL, DEMETER), (f) Nighttime total ion density data (IAP, DEMETER), (g) SST (NOAA), (h) AOD data (OMI), (i) AOD (Terra, MODIS), analysis using median method for Samoa earthquake.**

485

https://doi.org/10.5194/angeo-2021-41
Preprint. Discussion started: 1 September 2021


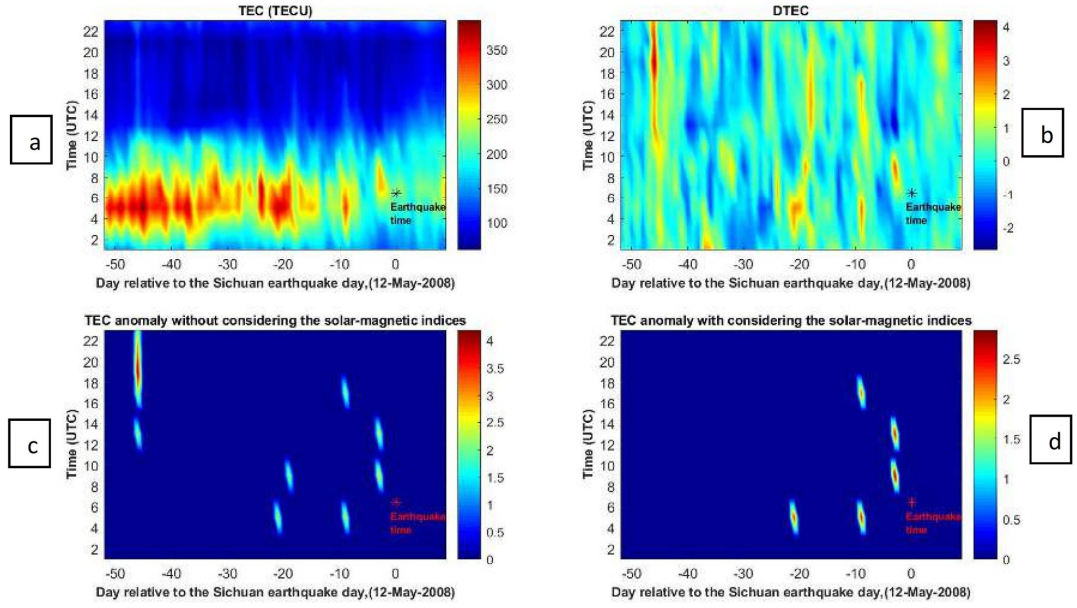


**Fig. 5. Results of TEC Analysis using median for Sichuan earthquake. The earthquake time is indicated by an asterisk. (a) TEC variations, (b) DTEC, (c) Detected anomalies without considering the solar-magnetic indices, (d) Detected anomalies with considering the solar-magnetic indices.**

490

https://doi.org/10.5194/angeo-2021-41
Preprint. Discussion started: 1 September 2021


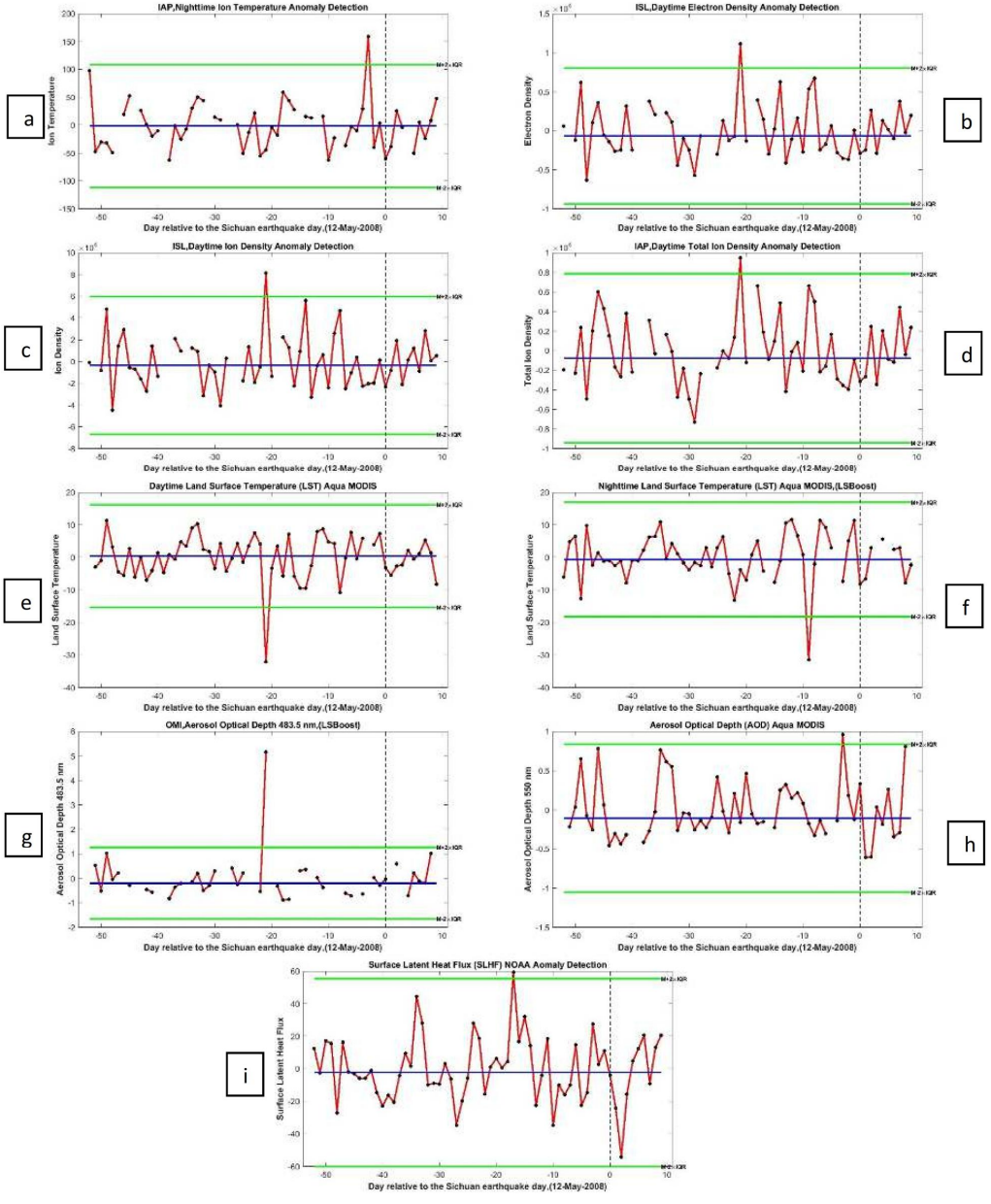


**Fig. 6. Results of (a) Nighttime ion temperature data (IAP, DEMETER), (b) Daytime electron density data (ISL, DEMETER), (c) Daytime ion density data (ISL, DEMETER), (d) Daytime total ion density data (IAP, DEMETER), (e) Daytime LST data (Aqua, MODIS), (f) Nighttime LST data (Aqua, MODIS), (g) AOD data (OMI), (h) AOD (Aqua, MODIS), (i) SLHF (NOAA), analysis using median method for Sichuan earthquake.**

https://doi.org/10.5194/angeo-2021-41
Preprint. Discussion started: 1 September 2021


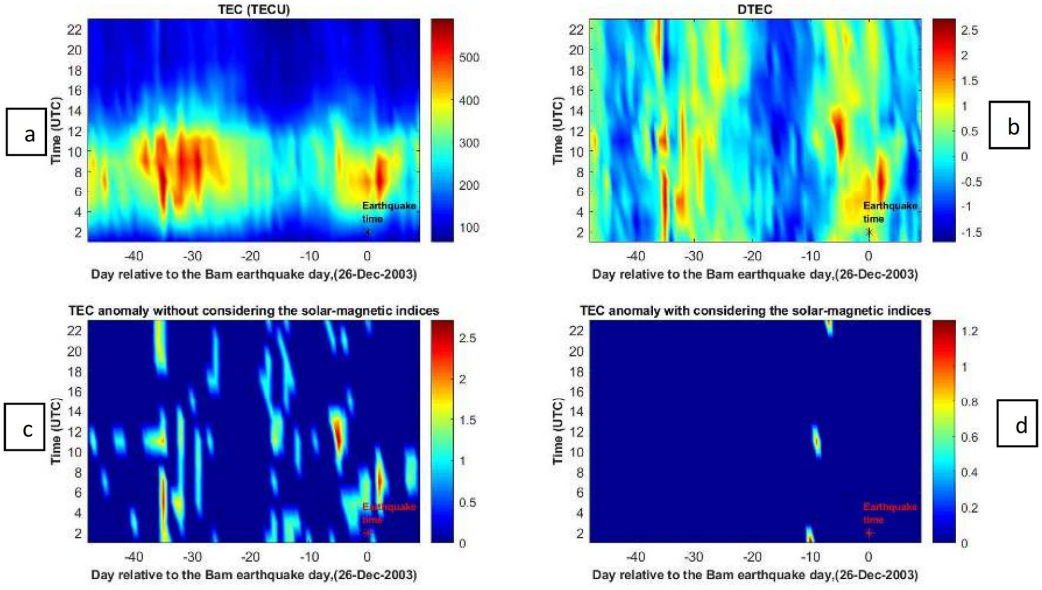


**Fig. 7. Results of TEC Analysis using median for Bam earthquake. The earthquake time is indicated by an asterisk. (a) TEC variations, (b) DTEC, (c) Detected anomalies without considering the solar-magnetic indices, (d) Detected anomalies with considering the solar-magnetic indices.**

https://doi.org/10.5194/angeo-2021-41
Preprint. Discussion started: 1 September 2021


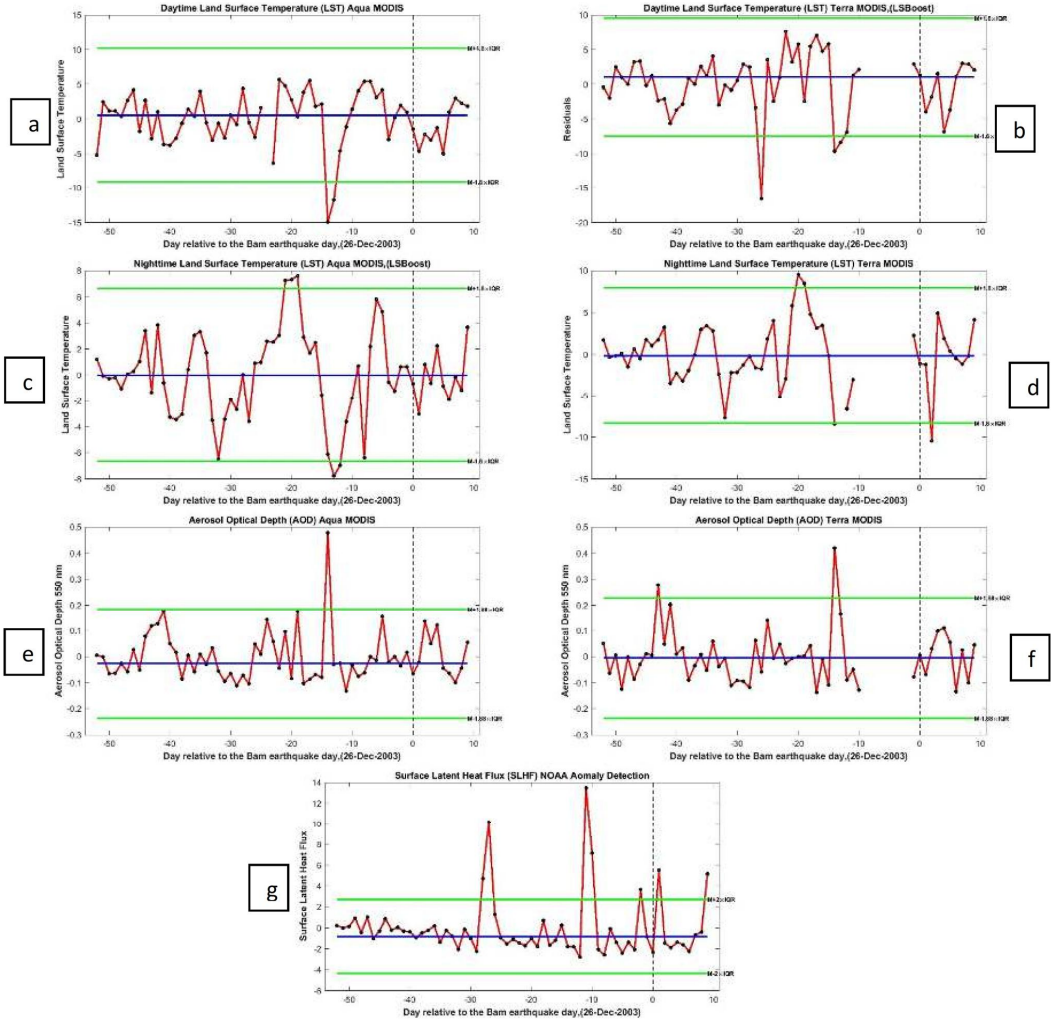


**Fig. 8. Results of (a) Daytime LST data (Aqua, MODIS), (b) Daytime LST data (Terra, MODIS), (c) Nighttime LST data (Aqua, MODIS), (d) Nighttime LST data (Terra, MODIS), (e) AOD data (Aqua, MODIS), (f) AOD (Terra, MODIS), (g) SLHF (NOAA), analysis using median method for Bam earthquake.**